EFDA–JET–CP(08)02/07

E. Nardon, A. Kirk, N. Ben Ayed, M. Bécoulet, G. Huysmans, P.R. Thomas,
H.R. Koslowski, Y. Liang, P. Cahyna, T.E. Evans
and JET EFDA contributors

ELM Control by Resonant Magnetic Perturbations on JET and MAST

ELM Control by Resonant Magnetic Perturbations on JET and MAST

E. Nardon[1], A. Kirk[1], N. Ben Ayed[1], M. Bécoulet[2], G. Huysmans[3], P.R. Thomas[3], H.R. Koslowski[3], Y. Liang[3], P. Cahyna[4], T.E. Evans[5] and JET EFDA contributors*

JET-EFDA, Culham Science Centre, OX14 3DB, Abingdon, UK

[1]EURATOM-UKAEA Fusion Association, Culham Science Centre, OX14 3DB, Abingdon, OXON, UK
[2]Association Euratom/CEA, CEA Cadarache, F-13108, St. Paul-lez-Durance, France
[3]Association Euratom/Forschungszentrum Jülich GmbH, IEF-4, Trilateral Euregio Cluster, D-52425, Jülich, Germany
[4]Institute of Plasma Physics AS CR v.v.i., Association EURATOM/IPP.CR, Prague, Czech Republic
[5]General Atomics, P.O. Box 85608, San Diego, California 92186, USA
** See annex of M.L. Watkins et al, "Overview of JET Results ", (Proc. 21[st] IAEA Fusion Energy Conference, Chengdu, China (2006)).*

Preprint of Paper to be submitted for publication in Proceedings of the HTPD High Temperature Plasma Diagnostic 2008, Albuquerque, New Mexico. (11th May 2008 - 15th May 2008)

ABSTRACT

In both JET and MAST, the Error Field Correction Coils (EFCCs) have been used recently in order to attempt to control Type I Edge Localised Modes (ELMs), which represent a major threat to the lifetime of plasma facing components in ITER. Using vacuum magnetic modelling it is suggested that the ELM mitigation observed at JET could be related to the ergodisation of the magnetic field at the edge. Indeed, the onset of ELM mitigation is found to be correlated with a certain level of the Chirikov parameter profile. Initial MAST results are presented which show an effect of EFCCs on the ELMs, again compatible with edge ergodisation according to the modelling. New coils dedicated to ELM control are ready for use on MAST this year and are presented here briefly.

1. INTRODUCTION

The control of Type I ELMs is recognised as essential for ITER in order to prevent damage to plasma facing components. One of the systems likely to be implemented on ITER for this purpose is a set of coils producing stationary non-axisymmetric magnetic perturbations. Experiments at DIII-D have demonstrated that two rows of off mid-plane in-vessel coils (I-coils) producing n=3 perturbations (n being the toroidal mode number) could suppress ELMs [1].

More recently, experiments have been performed on JET [4,5] and MAST using Error Field Correction Coils (EFCCs). The EFCCs design is similar in these two machines (and somewhat different from the DIII-D I-coils design), with four large rectangular coils located outside the vacuum vessel, capable of producing either n=1 or n=2 perturbations. Instead of full ELM suppression, JET experiments have demonstrated a strong reduction in ELM size and increase in ELM frequency induced by the EFCCs, as reported in [4,5]. MAST results are more preliminary but a similar effect was observed in some cases, as will be shown here.

Generally speaking, the precise mechanisms leading to ELM control remain unclear, and it is essential in view of ITER to progress in their comprehension. It was suggested that the ergodisation of the magnetic field at the edge by Resonant Magnetic Perturbations (RMPs) from the coils could be a key element [1,4-6]. Edge ergodisation is actually used as a criterion for designing the ITER ELM control coils [2,3,8].

In this paper, we discuss some aspects of the experimental results from JET (section 2) and MAST (section 3) and their relation to the predictions of edge ergodisation. This is done in the frame of a vacuum modelling which makes use of the ERGOS code, presented in [2,3]. The vacuum approximation consists in neglecting the plasma magnetic response to the magnetic perturbations (for instance the screening of the RMPs due to plasma rotation). This strong assumption is used for its simplicity rather than on the basis of physical arguments (models for the plasma response are under progress [2,3,9]). Finally, in section 4, we present the new MAST coils dedicated to ELM control which will be used for the first time in 2008.

2. JET EFCCS N=1 EXPERIMENTS

In the 2006/2007 JET ELM control experiments with EFCCs in a n=1 configuration [4,5], the EFCCs pulse usually began with a ramp up phase over several tenths of second. It was clearly observed that ELM mitigation did not start at the very beginning of the EFCCs pulse, but only after a certain delay. Although shot-to-shot scans or slower ramps of the EFCCs current I_{EFCC} would be required to confirm the existence of a threshold effect, here a "threshold current" ($I_{EFCC,thr}$) is defined as the value of I_{EFCC} at the onset of ELM mitigation. It was found that $I_{EFCC,thr}$ depends on the discharge characteristics [4,5]. Fig. 1 shows the Chirikov parameter ($_{Ch}$, see definition in [3]) profiles calculated with ERGOS [2,3] for a set of four discharges which differ in particular by the value of q_{95} (ranging from 3.0 to 4.8) (see Fig. 5 in [5]). The Chirikov parameter quantifies the degree of island overlapping and is thereby an indicator of ergodicity. A typical n=3 DIII-D case, where complete ELM suppression was obtained, as well as the MAST EFCCs n=2 case described in section 3 are also shown for comparison. The left plot shows the ERGOS results for I_{EFCC}=32kAt for all the JET discharges. This was the maximal current allowed by the power supplies during these experiments; however, this value could not be reached in all four discharges due to locked modes in the lower q95 cases. The disparity between the JET discharges is a consequence of the fact that $_{Ch}$ depends on the pitch angle of the field lines as well as on the magnetic shear, which both vary with q_{95}. Discharges with a larger q_{95} typically have a larger $_{Ch}$. The right plot in Fig. 1 corresponds to calculations done for I_{EFCC}=$I_{EFCC,thr}$ for each JET discharge. In that case, the JET profiles are observed to overlap. This suggests that $_{Ch}$ could be a key parameter in these experiments and therefore that ergodicity could be playing a central role. The interpretation of this result is however not straightforward, because $_{Ch}$ is well defined only at discrete locations (in the middle between each pair of neighbouring n=1 islands chains) which differ from one discharge to another, and the meaning of a $_{Ch}$ *profile* is not clear. Another remark to make is that for I_{EFCC}=$I_{EFCC,thr}$, $_{Ch}$ is slightly below 1, i.e. the n=1 islands chains do not overlap. It can thus be questioned whether the edge magnetic field is really ergodised. Fig. 2 presents a Poincaré plot for one of the cases appearing in Fig. 1. It is obtained by following a large number of field lines for up to 8000 toroidal rotations. The colour of the points is determined by the number of turns after which a field line crosses the unperturbed separatrix. Field lines failing to cross the separatrix receive the colour corresponding to 8000. It can be seen that the region spanned by field lines that cross the unperturbed separatrix within 8000 toroidal rotations (in fact much less than that for most of them) extends beyond the 4/1 islands chain. A more detailed study shows that the 4/1 and 5/1 islands chains do not overlap, consistent with $_{Ch}$<1, but that a 9/2 chain of secondary islands fills the gap in-between them. This conforms to [7], where the condition $_{Ch}$>2/3 is stated as a more accurate criterion than $_{Ch}$>1 for ergodicity to appear, due to secondary islands chains.

Coming back to Fig. 1, we see that in the pedestal region ($\psi_{pol}^{1/2} > 0.95$ typically) none of the JET shots reached values of $_{Ch}$ equal to the DIII-D case. More inwards ($\psi_{pol}^{1/2} \approx 0.9$) however, the highest JET shot reached the DIII-D value. In that case, the ergodised region (i.e. the region satis-

fying $_{Ch}$>2/3) is about as broad in JET as in DIII-D. Unlike in DIII-D, full ELM suppression was not obtained at JET, even in that discharge. This is an indication that the width of the ergodised region is not the only parameter controlling complete ELM suppression, or that the plasma magnetic response is different between the two machines.

3. PRELIMINARY EXPERIMENTAL RESULTS ON MAST USING THE EFCCS

In 2007, MAST also used EFCCs in order to try and mitigate ELMs. Fig. 3 shows the results obtained by applying a n=2 perturbation in a low collisionality discharge (reference discharge: #17919, double null plasma with 1.7MW of neutral beam heating [single beam], plasma current I_p=750kA and toroidal magnetic field on the magnetic axis [R_{mag}=0.92m] B_t=-0.52T), using EFCCs currents of I_{EFCC}=0 (for reference), 12, and 15kAt. Notice that the ELMs in this type of discharge have a high natural frequency (~500Hz) and cannot be classified as Type I ELMs. Nevertheless, the EFCCs were observed to increase their frequency by typically 25%. The evolution of the line integrated density shows that the EFCCs enhance the rate of density drop (without EFCCs, these plasmas have a naturally decreasing density). This is reminiscent of the density pump-out observed in experiments on DIII-D and JET [1,4,5]. The $_{Ch}$ profile for the case with I_{EFCC}=15kAt is presented on Fig. 1 and is clearly above the DIII-D and JET profiles. This is due to the large magnetic shear at the edge of MAST, which supports the overlapping of islands. From the edge ergodisation criterion, a suppression of the Type I ELMs could therefore be expected. The fact that ELM suppression is not observed here could be due to the fact that these ELMs are not Type I ELMs, but also to the insufficiency of the vacuum modelling, or to the fact that edge ergodisation by itself is not sufficient for ELM suppression.

4. PRESENTATION OF THE NEW MAST ELM CONTROL COILS

Starting in 2008, MAST will be able to enhance significantly its contribution in the domain of ELM control by RMPs, thanks to the installation of twelve “I-like coils” (i.e. internal off mid-plane coils producing n=3 perturbations) dedicated to ELM control. Their layout is presented in Fig. 4. Profiles of $_{Ch}$ calculated for a typical MAST equilibrium and for a current of 5.6kAt (maximal current allowed by the power supplies), are shown in Fig. 5. The coils can produce $_{Ch}$>1 for $\psi_{pol}^{1/2} > 0.91$, which is slightly better than the MAST EFCCs in a n=2 configuration, and clearly better than the I-coils on DIII-D or the EFCCs on JET. Fig. 5 presents a study of the effect on $_{Ch}$ of taking into account the bootstrap current in the equilibrium reconstruction. The interest of this study is that the bootstrap current typically flattens the q profile in the pedestal region, reducing $_{Ch}$ by making the islands chains more distant from each other, which could prevent edge ergodisation. The quantitative analysis appearing in Fig. 5 shows that this effect exists but is small: $_{Ch}$ remains well above 1 in the bootstrap region, even if an artificial level of bootstrap 3 times larger than the one expected from profiles measurements is imposed.

5. CONCLUSION

Vacuum modelling with ERGOS for the JET EFCCs n=1 experiments shows a correlation between the onset of ELM mitigation and the $_{Ch}$ profile, suggesting that edge ergodisation could be playing a key role in ELM mitigation. This result needs to be confirmed by analysing more shots and making proper I_{EFCC} scans to verify the threshold effect. On MAST, results obtained with the EFCCs in a n=2 configuration show an effect on the ELMs. The Chirikov parameter is greater in MAST than in DIII-D and JET, again pointing to edge ergodisation as a potential mechanism. New coils dedicated to ELM control have been installed recently on MAST. They were designed to be able, in the vacuum approximation, to ergodise a broad region at the edge of the plasma. They will be used for the first time in 2008. Finally, it should be stressed that the vacuum approximation was used mainly for its simplicity. Present models for the plasma response [2,3,9] suggest however that the plasma response has a significant role, in particular inside the pedestal. Nevertheless vacuum modelling is so far the only method of comparison between the different machines. decreases from 3% to 2%. Experimentally, the inter-ELM H-Mode plasmas have a factor-of-two higher sputtering yields which was not correlated to the applied power, the plasma current, or the beam energy. Again, the inter-ELM H-Mode EDGE2D calculation also had a factor of two higher sputtering yields than L-Mode (star point in figure 5). This indicates that time evolution and pedestal effects are the likely origin of the larger sputtering yield.

ACKNOWLEDGEMENTS

UKAEA authors were funded jointly by the United Kingdom Engineering and Physical Sciences Research Council and by the European Communities under the contract of Association between EURATOM and UKAEA. The views and opinions expressed herein do not necessarily reflect those of the European Commission.

REFERENCES

[1]. T.E. Evans, *et al*., Nucl. Fusion **48** (2008) 024002

[2]. M. Bécoulet, *et al*., Nucl. Fusion **48** (2008) 024003

[3]. E. Nardon, *et al*., Nucl. Fusion **363-365** (2007) 1071

[4]. Y. Liang, *et al*., Phys. Rev. Lett **98** (2007) 265004

[5]. Y. Liang, *et al*., Plasma Phys. Control. Fusion **49** (2007) B581

[6]. M.E. Fenstermacher, *et al*., Phys. Plasmas **15** (2008) 056122

[7]. A.J. Lichtenberg and M.A. Lieberman, *et al*., "Regular and Stochastic Motion", Applied Mathematical Sciences **38**, Springer-Verlag, New York Heidelberg Berlin, (1983)

[8]. M.J. Schaffer, *et al*., Nucl. Fusion **48** (2008) 024004

[9]. M.F. Heyn et al., Nucl. Fusion **48** (2008) 024005

FIGURES

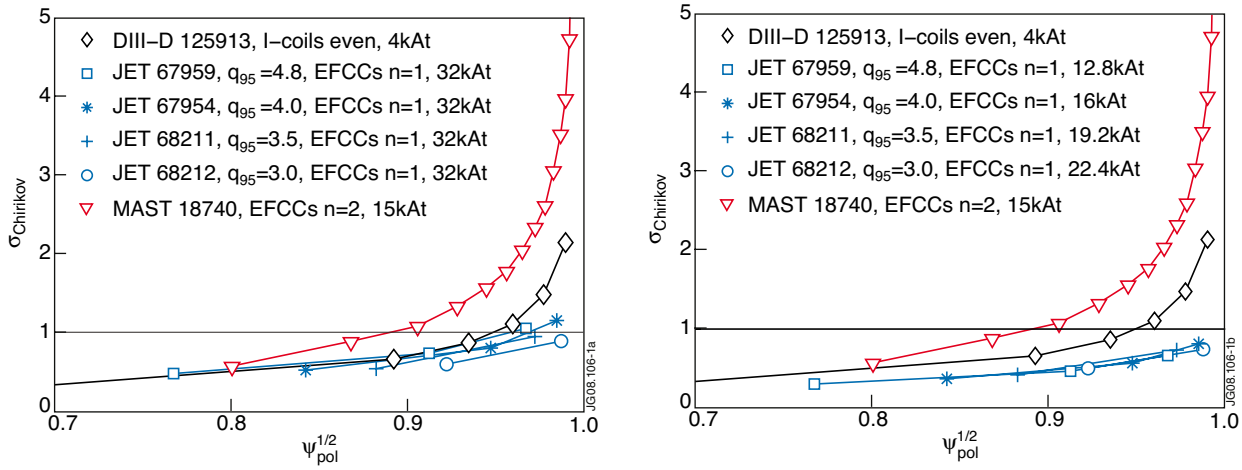

Figure 1. Calculated profiles of the Chirikov parameter for JET, MAST and DIII-D. The four JET profiles are for the EFCCs in a n=1 configuration and discharges with different q_{95} values. In the left plot IEFCC=32kAt and in the right plot $I_{EFCC}=I_{EFCC,thr}$. The MAST profile corresponds to the experiments presented in section 3, with EFCCs in a n=2 configuration. The DIII-D profile corresponds to a typical discharge where complete ELM suppression was obtained.

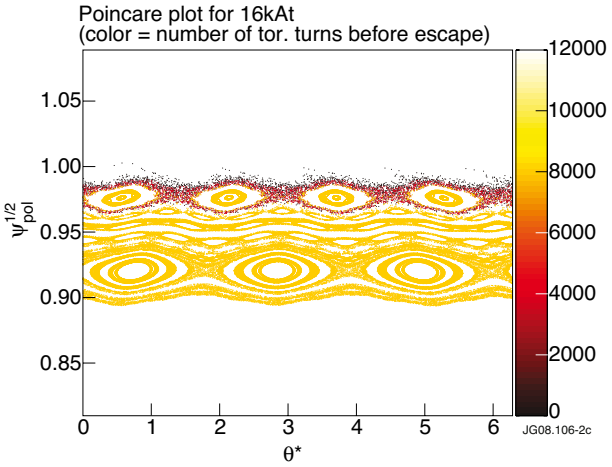

Figure 2. Poincaré plot for JET discharge 67954 (q_{95}=4.0) for $I_{EFCC}= I_{EFCC,thr}$.

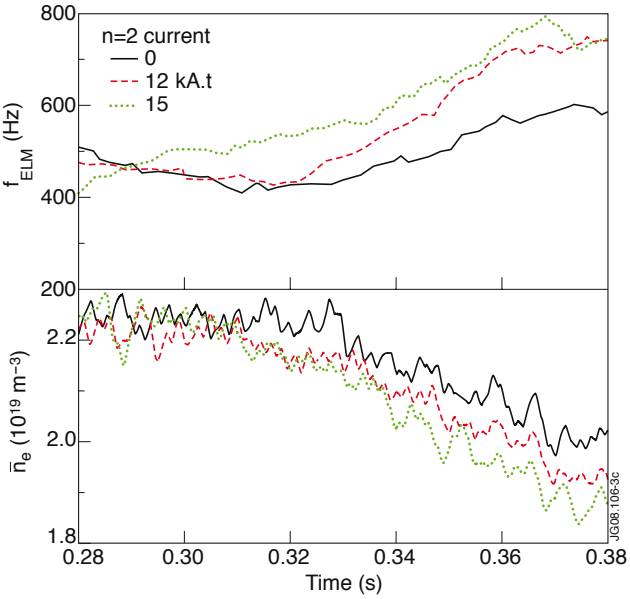

Figure 3. ELM frequency and line integrated density in MAST low pedestal collisionality (ν_e^*=0.3) plasmas where the EFCCs were applied in a n=2 configuration with currents of 0, 12 and 15kAt.

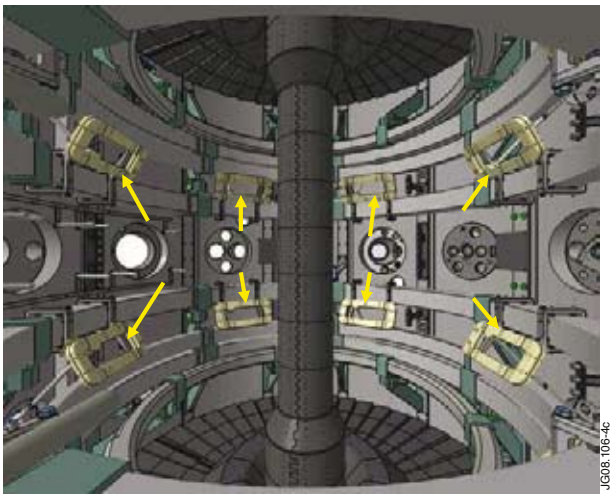

Figure 4. The new MAST ELM control coils (only 8 of the 12 coils are visible here and they are indicated by arrows).

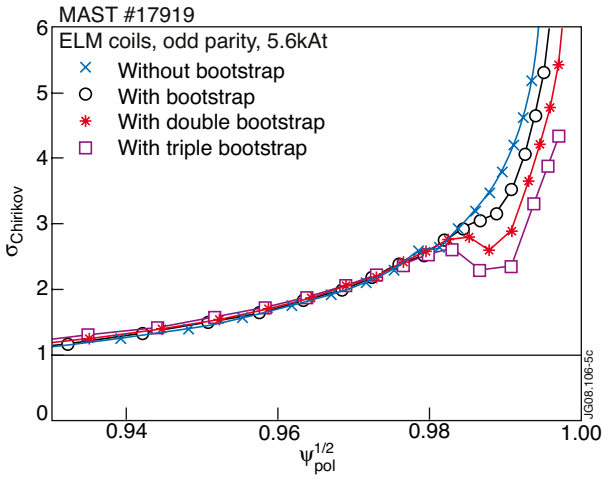

Figure 5. Predicted profiles of the Chirikov parameter produced by the new MAST ELM control coils in odd parity configuration (i.e. currents in the coils flow in such a way that the radial perturbation produced by a given upper coil has an opposite sign to the one produced by the lower coil at the same toroidal location), showing the effect of varying the amplitude of the bootstrap current in the equilibrium reconstruction.